www.czasopisma.pan.pl PAN POLSKA AKADEMIA NAUK www.journals.pan.pl

Arch. Metall. Mater. **66** (2021), 2, 627-635

DOI: 10.24425/amm.2021.135900

CHANDRU MANIVANNAN[1*], SELLADURAI VELAPPAN[2], VENKATESH CHENRAYAN[3]

MULTIOBJECTIVE PERFORMANCE INVESTIGATION OF CNT COATED HSS TOOL UNDER THE RESPONSE SURFACE METHODOLOGY PLATFORM

The present research employs the statistical tool of Response surface methodology (RSM) to evaluate the machining characteristics of carbon nanotubes (CNTs) coated high-speed steel (HSS) tools. The methodology used for depositing carbon nanotubes was Plasma-Enhanced Chemical Vapor Deposition (PECVD). Cutting speed, thickness of cut, and feed rate were chosen as machining factors, and cutting forces, cutting tooltip temperature, tool wear, and surface roughness were included as machining responses. Three-level of cutting conditions were followed. The face-centered, Central Composite Design (CCD) was followed to conduct twenty number of experiments. The speed of cutting and rate of feed have been identified as the most influential variables over the responses considered, followed by the thickness of cut. The model reveals the optimized level of cutting parameters to achieve the required objectives. The confirmation experiments were also carried out to validate the acceptable degree of variations between the experimental results and the predicted one.

Keywords: Carbon nanotube, RSM, cutting forces, cutting tooltip temperature, tool wear

1. Introduction

The conventional way used for machining of hard materials involves rough turning, followed by grinding, which results in increased production time and expense. On the other hand, the process of hard turning removes the cost of lubrication and decreases the production time relative to grinding. Machining industries are now concentrating on dry as well as semi-dry machining to minimize the expense of cutting fluids, which in turn significantly reduces the production costs. The absence of cutting fluids will also help the operator to escape from skin problems such as cold burns, allergy, etc., and asphyxiation in the case of coolants under cryogenic conditions [1]. In these situations, the tool wear is an important criterion to be observed since the tool wear will be greater during dry machining at elevated cutting temperature, resulting in a rapid tool failure. To address the issue, most of the recent researchers were developed cutting tools with various coating like TiAlN, TiN, TiCrN, etc. This particular research investigates the performance of the CNT coated tool targeting multi-response through a mathematical model.

The effect of machining parameters on turning of AISI D3 cold-worked tool steel with ceramic inserts CC650 and CC6050 was investigated by Hamza Bensouilah et al. [2]. The tests were based on the orthogonal array L_{16} of Taguchi. Analysis of variance (ANOVA) and RSM were employed to measure the optimal process parameters. The surface quality attained by CC6050 coated ceramic insert is 1.6 times the quality achieved by CC650 uncoated ceramic insert. The behavior of tool wear and cutting forces of cubic boron nitride tool during turning of bearing steel AISI 52100 was examined by Khaider Bouacha et al. [3]. The relationship between the input and output parameters was modeled by using RSM and the joint effect has been studied through ANOVA. The findings revealed that the thrust force is highly susceptible to the hardness of the workpiece. While turning iron-nickel based superalloy with carbide TiAlN coated tool, the impact of the cutting parameters on the tool life and the volume of work material removed was assessed by Behnam Davoodi et al. [4]. The interactions between machining input parameters and output response variables were formed by RSM and ANOVA was carried out to ensure the mathematical model's adequacy. The author noticed that the cutting speed

[1] DHIRAJLAL GANDHI COLLEGE OF TECHNOLOGY, SALEM – 636309, TAMILNADU, INDIA
[2] COIMBATORE INSTITUTE OF TECHNOLOGY, COIMBATORE – 641014, TAMILNADU, INDIA
[3] ADAMA SCIENCE AND TECHNOLOGY UNIVERSITY, ADAMA, ETHIOPIA

* Corresponding author: mechchandru123@gmail.com

was the major determinant factor for tool life. J.S. Dureja et al. [5] tested the tool wear and surface roughness while machining steel AISI D3 with TiSiN/TiAlN coated carbide tools. Taguchi's orthogonal array of $L9(3)^3$ and RSM were used to refine input parameters so that roughness and wear were minimized. Ashvin J. Makadia et al. [6] have developed a surface roughness prediction model based on RSM to find the effects of major turning parameters during machining of steel AISI 410. The prediction equation built reveals that the feed rate is the key impact factor for surface roughness, followed by the tool nose radius. M. Nalbant et al. [7] utilized Taguchi's technique in optimizing the machining parameters while turning steel AISI 1030 with TiN coated inserts. M.Y. Noordin et al. [8] examined the performance behavior of tools coated with tungsten carbide while machining steel AISI 1045 with the help of RSM. It was also found that the most powerful factor influencing tangential force and surface roughness is the feed, nevertheless the interaction between feed and side cutting edge angle also contribute to surface roughness. Anderson P. Paiva et al. [9] presented a hybrid approach of principal component analysis and RSM in optimizing the process parameters for turning steel AISI 52100. In the hard turning of steel AISI 4340 with uncoated and multi-layer coated carbide tools, Ashok Kumar Sahoo et al. [10] analyzed the cutting forces, chip morphology, flank wear and surface roughness through ANOVA.

Pazhanivel et al. [11] conducted an experiment to examine the machinability and wear behavior of CNT coated inserts. The findings proved that the friction coefficient of the multi-walled carbon nanotubes (MWCNT) coated inserts decreased significantly, resulting in improved machinability with enhanced surface finish. The sliding friction characteristics of CNTs were analyzed on silicon, silicon nitride, and cemented carbide substrates by Atsushi Hirata et al. [12]. The results showed that the CNTs coated over surface porosity substrates had greater lubrication and higher adhesive strength. T. Borkar et al. [13] explored the findings that the pulsed electrode deposition CNT coating increases the tribology property than the pure nickel coatings. The mechanical properties of single and multi-walled carbon nanotubes were investigated by J.P. Salvetat et al. [14]. The Young's modulus of smaller SWCNTs is greater than graphite and the degree of order in the walls of the tube greatly affects the Young's modulus of MWCNTs.

In this research work, the attempt has been made to deposit the novel CNTs through PECVD technique, over the commonly used cutting tool made of HSS. But as far as the workpiece is concerned, poor thermal conductivity, retaining the hardness even at elevated temperature and chemical reactivity are the main factors which make Titanium alloy to be as low machinability material. This novel coating was initiated to bridge the gap between low machinability material and dry machining. The extension of this research work is aiming to optimize the machining parameters and analyzes the statistically significant cutting parameter with respect to tool wear and workpiece quality.

2. Materials and methods

2.1. CNT Coating procedure

Carbon Nanotubes (CNTs) were coated over the HSS tool substrates by PECVD technique using Roth & Rau microsystems, HBS 500, Germany equipment. Initially, the substrates over which the CNTs are to be grown were cleaned with the aid of an ultrasonic cleaner for about 20 minutes to clean dirt, dust, and foreign particles present over the surface of the substrates. Before attempting the CNT deposition, a thin nickel film was deposited on the HSS substrate by the DC sputtering technique, which acts as a catalyst for the development of CNTs.

2.2. Characterization of CNT deposition

The HORIBA LabRAM HR Evolution spectrometer under 532 nm backscattering excitation wavelength is used to acquire the micro-Raman spectrum of the CNT-coated layer to acknowledge the presence of CNTs in the coating. Zeiss Sigma Field Emission Scanning Electron Microscope (FE-SEM) from Carl Zeiss was used to analyze surface characteristics of the CNT coating. Clear images of coated carbon nanotubes with smaller aspect ratios were observed from Fig. 1(a) and Fig. 1(b).

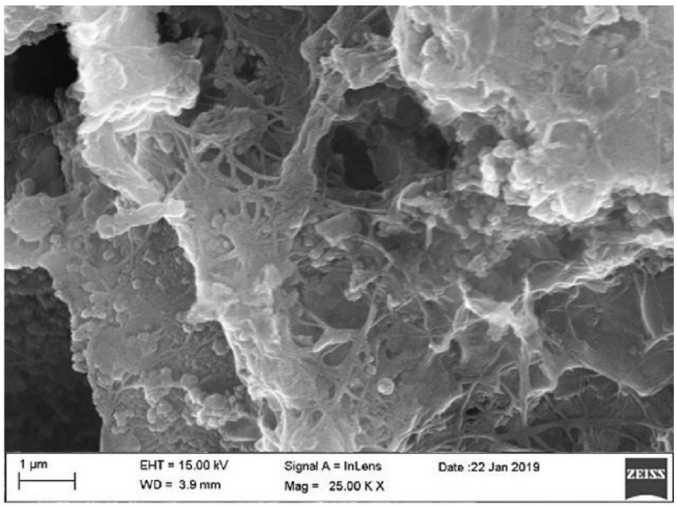

Fig. 1(a). SEM image of CNT deposition over HSS substrate at 25K × magnification

A scratch test was also performed with the help of Ducom scratch wear testing machine to ascertain the adhesive strength of the CNT coating with the substrate material. In this experiment, a 0.2 mm radius diamond stylus indenter is pushed over a coated specimen surface with a stroke length of 6 mm at 0.2 mm/s traction speed. The adhesive strength of the coating with the substratum has been obtained from the following Eq. (1) as 660 N/mm^2, which is almost 3/4th yield strength of substrate, nearly 900 N/mm^2.

$$\sigma_A = \frac{2W_c}{\pi Rb} \tag{1}$$

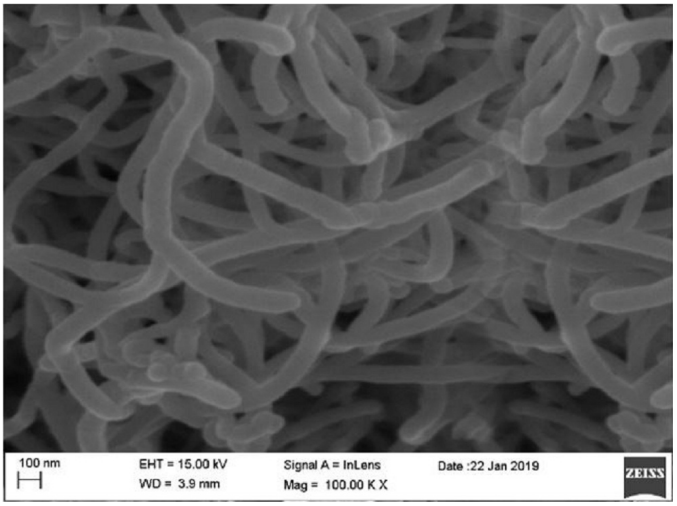

Fig. 1(b). SEM image of CNT deposition over HSS substrate at 100K × magnification

2.3. Experimental details

The CNC lathe (Jobber LM, ACE micromatic) was used as a machining resource. A 50 mm diameter and 150 mm long Titanium alloy commercial-grade 5 rod has been used as a working material for machining experiments. The HSS tools used for machining the titanium alloy were coated with CNTs as described earlier.

Three different cutting conditions were followed during the experiment as shown in Table 1. The cutting force, cutting tooltip temperature, tool wear, and surface roughness were considered as machining objectives.

TABLE 1

Experimental cutting parameters

Parameter / Level	Level 1	Level 2	Level 3
Cutting Speed (m/min)	250	350	450
Thickness of cut (mm)	0.3	0.5	0.8
Feed rate (mm/rev)	0.2	0.25	0.3

2.4. Measurement of objectives

2.4.1. Cutting tooltip temperature

The FLIR E50 thermal imaging camera was used for temperature evaluation in the cutting zone during the turning process. The thermal image camera has an auto-orientation feature, 3.1 MP IR resolution, and 0.050°C thermal sensitivity. It is capable to record –20°C to 1000°C. A special fixture was employed to adjust the focal height and angle, to get the precise measurement and was fixed over the bed of the machine.

2.4.2. Cutting forces

The cutting forces were calculated using a KISTLER 5697A dynamometer and DyanoWare data acquisition program by maintaining a cutting time of 60 sec for each trial.

2.4.3. Surface roughness

MITUTOYO SJ 410 surface roughness tester was used to assess the surface roughness (Ra). With each experiment, the readings were recorded at three different positions across the circumference of the workpiece at 120° by keeping 4 mm as trace length.

2.4.4. Tool wear

The Atomic Force Microscope (NTEGRA, NTMDT, Russia) and DINO-LITE digital Optical Microscope with 640 × 480-pixel resolution, magnification range from 10× to 230×, and frame rate of 30 FPS were used to analyze wear growth under all cutting conditions.

2.5. Development of mathematical model

A mathematical model can be developed by including independent process variables in a quantifying form to represent a response is as follows in Eq. (2).

$$Y = cf^{p}v^{q}d^{r} \tag{2}$$

where, Y – the predicted response, c – the constant, v – the speed of cutting (m/min), f – the rate of feed (mm/rev), and d – the thickness of cut (mm). The constants to be derived are p, q, and r.

The above-stated equation can be transformed through logarithmic transformation, to convert the nonlinearity into linear form and represented in Eq. (3).

$$\ln(Y) = \ln c + \ln pf + \ln qv + \ln rd \tag{3}$$

This is one of the analytical modeling techniques for data transformation, the same can be rewritten as mentioned in Eq. (4).

$$\varnothing = \beta_0 + \beta_1 x_1 + \beta_2 x_2 + \beta_3 x_3 \tag{4}$$

where, $\varnothing$ is the actual value of predicted response on the logarithmic scale, it can also be rewritten in a simple way as represented in Eq. (5).

$$\bar{y} = b_0 + b_1 x_1 + b_2 x_2 + b_3 x_3 \tag{5}$$

where, $\bar{y}$ is the value of predicted response after the logarithmic transformation. b_3, b_2, b_1, and b_0 are the measures of the parameters β_3, β_2, β_1, and β_0 respectively. Estimation of these three parameters through analyzing the experimental data can

be done in either first-order or second-order quadratic model, the developed quadratic model is given in Eq. (6).

$$\tilde{y} = \beta_0 + \beta_1 V + \beta_2 f + \beta_3 d + \beta_{11} V^2 + \\ + \beta_{22} f^2 + \beta_{33} d^2 + \beta_{12} Vf + \beta_{13} Vd + \beta_{23} fd \quad (6)$$

The estimated response is correlated with a set of regression coefficients, intercepts (β_0) linear ($\beta_1, \beta_2, \beta_3$), quadratic ($\beta_{11}, \beta_{22}, \beta_{33}$), and interaction ($\beta_{12}, \beta_{13}, \beta_{23}$).

2.6. Response surface methodology

RSM is a mixture of statistical and mathematical approaches used to model and analyze the problem in which the objectives are influenced by several variables. RSM is also applying the techniques of quantification of the relationship between responses and important variables.The design expert (version 11) software was employed to build the RSM experimental plan. To analyze the experimental results, the same software was also used by the following the step sequence: (i). Prefer the transformation, if needed, otherwise select none option. (ii). Select the right model by verifying the Fit summary tests like the F-test and lack of fit test. (iii). Manipulate the ANOVA and the results of individual responses to validate the adequacy of the model with help of R^2 Adj R^2 value. (iv). Utilize the various plots like residual plot, residual vs. predicted plot, to authenticate the suitability of the model proposed. (v). If the model seems to be adequate, generate 3D contour graphs, interaction plots to interpret the effect of variables over the responses considered.

3. Results and discussion

Nearly 20 number of experiments were performed as per the design matrix drawn from RSM. The machining experiments were analyzed in the central composite design (CCD) concept with a face-centered cubic. A full factorial design that combines all factors on two levels. As a face-centered cubic, a star point locating on the face of the cube section corresponds to the α value of 0 as a midpoint. The upper and lower value of α as +1 and –1 respectively. The mid-value of the factors, considered were arrived accordingly as feed rate of 0.25 mm/rev, cutting speed of 350 m/min, and thickness of cut of 0.55 mm.

Table 2 shows the sequence of 20 number of experiments conducted as per the design matrix and their corresponding responses were recorded. Each response value was recorded for all the experimental runs, and its analysis shows that the quadratic model is a recommended one, by fulfilling all the components of fit summary test.

3.1. ANOVA Analysis

It is quite obvious that the proposed model should be validated with various indicators like significance of the regression model, significance of the individual coefficient of the model, test for lack of fit an adequacy precision, etc. An ANOVA table shown for the responses considered was employed to validate the adequacy of the proposed model with the aid of the above-said indicators. If the value of p is below 0.05, the model is guaranteed to be significant [8]. The lack of fit test insignifi-

TABLE 2

Experimental results

Std.	Run	Factor 1 A:Cutting Speed (m/min)	Factor 2 B:Feed (mm/rev)	Factor 3 C: Thickness of cut (mm)	Response 1 Cutting tooltip temperature (°C)	Response 2 Cutting force (N)	Response 3 Surface Roughness (µm)	Response 4 Tool wear (mm)
15	1	350	0.25	0.55	112.5	227.65	0.878	0.195
7	2	250	0.3	0.8	99.52	167.25	0.687	0.175
1	3	250	0.2	0.3	95	159.2	0.603	0.165
8	4	450	0.3	0.8	128	243.75	1.089	0.228
10	5	450	0.25	0.55	125.67	232.65	1.012	0.223
3	6	250	0.3	0.3	98.1	163.25	0.656	0.168
19	7	350	0.25	0.55	112.75	225.45	0.895	0.192
4	8	450	0.3	0.3	127.6	240.15	1.045	0.221
2	9	450	0.2	0.3	126.9	229.43	0.978	0.22
20	10	350	0.25	0.55	112.85	224.75	0.89	0.191
6	11	450	0.2	0.8	127.5	228.75	1.023	0.226
12	12	350	0.3	0.55	115.13	231.56	0.901	0.193
5	13	250	0.2	0.8	98.25	158.54	0.645	0.171
13	14	350	0.25	0.3	114.75	224.75	0.837	0.189
14	15	350	0.25	0.8	113.75	231.15	0.899	0.199
9	16	250	0.25	0.55	96	155.65	0.661	0.173
17	17	350	0.25	0.55	113	228.24	0.891	0.192
18	18	350	0.25	0.55	113.25	226.84	0.798	0.19
16	19	350	0.25	0.55	112.55	227.47	0.893	0.191
11	20	350	0.2	0.55	112.15	224.36	0.845	0.188

cancy is mandatory for any model. The closest value of R^2 to 1 and the existence of good agreement between predicted R^2 and adjusted R^2 (difference between them is less than 0.02) are the preferable scale of adequacy. The value of adequacy precision greater than 4 assures the developed model is quite adequate.

Table 3 shows the ANOVA analysis for the response cutting tooltip temperature. The table content confirms that the conditions of important indicators like model significance, lack of fit, R^2, Adj R^2, and adequacy precision are in good agreement. The cutting tooltip temperature is highly influenced by the impact of cutting speed by nullifying the influence of the rest of the parameters. Similarly, Table 4, Table 5 and Table 6 show the analysis of ANOVA for the responses cutting force, surface roughness, and tool wear respectively, which has reasonable agreement with necessary indicators by proving the suitability of the model.

Table 4 shows the ANOVA analysis for the cutting force response, which highlights the fact that the cutting force was greatly influenced by the speed of cutting followed by the rate of feed. Similar results were achieved by the researchers K. Bouacha et al. [3]. Table 5 shows the ANOVA analysis for the surface roughness which reveals that the considered response was greatly influenced by the cutting speed by exhausting the effect of other parameters [6]. Table 6 shows the ANOVA analysis of the tool wear, which confirms that the wear of the tool was considerably

TABLE 3

ANOVA (Reduced model) for cutting tooltip temperature

Source	Sum of Squares	df	Mean Square	F-value	p-value	—	PCR
Model	2235.98	5	447.20	712.12	<0.0001	significant	—
A-Cutting Speed	2214.14	1	2214.14	3525.84	<0.0001	—	99.00
B-Feed	7.31	1	7.31	11.64	0.0042	—	0.33
C-Thickness of cut	2.18	1	2.18	3.47	0.0835	—	0.01
A^2	11.73	1	11.73	18.68	0.0007	—	0.52
C^2	3.57	1	7.21	11.47	0.0044	—	0.14
Residual	8.79	14	0.6280			—	—
Lack of Fit	8.39	9	0.9326	11.71	0.0073	significant	—
Pure Error	0.3983	5	0.0797	—	—	**R^2**	0.9961
Cor Total	2244.77	19	—	—	—	**Adj R^2**	0.9947

TABLE 4

ANOVA (Reduced model) for cutting force

Source	Sum of Squares	df	Mean Square	F-value	p-value		PCR
Model	18332.72	6	3055.45	806.39	<0.0001	significant	—
A-Cutting Speed	13752.23	1	13752.23	3629.45	<0.0001	—	75.02
B-Feed	208.67	1	208.67	55.07	<0.0001	—	1.14
C-Thickness of cut	16.03	1	16.03	4.23	0.0604	—	—
AB	21.00	1	21.00	5.54	0.0350	—	—
A^2	3080.91	1	3080.91	813.10	<0.0001	—	16.8
B^2	24.75	1	24.75	6.53	0.0239	—	—
Residual	49.26	13	3.79	—	—	—	—
Lack of Fit	40.01	8	5.00	2.71	0.1440	not significant	—
Pure Error	9.24	5	1.85			**R^2**	0.9973
Cor Total	18381.98	19				**Adj R^2**	0.9961

TABLE 5

ANOVA (Reduced model) for surface roughness

Source	Sum of Squares	df	Mean Square	F-value	p-value	—	PCR
Model	0.3776	4	0.0944	173.87	< 0.0001	significant	
A-Cutting Speed	0.3591	1	0.3591	661.47	< 0.0001	—	95.1
B-Feed	0.0081	1	0.0081	14.86	0.0016	—	—
C-Thickness of cut	0.0050	1	0.0050	9.24	0.0083	—	—
A^2	0.0054	1	0.0054	9.91	0.0066	—	—
Residual	0.0081	15	0.0005			—	—
Lack of Fit	0.0010	10	0.0001	0.0704	0.9997	not significant	—
Pure Error	0.0071	5	0.0014	—	—	**R^2**	0.9789
Cor Total	0.3857	19	—	—	—	**Adj R^2**	0.9733

TABLE 6

ANOVA (Reduced model) for tool wear

Source	Sum of Squares	df	Mean Square	F-value	p-value	—	PCR
Model	0.0074	4	0.0018	595.52	<0.0001	significant	—
A-Cutting Speed	0.0071	1	0.0071	2292.31	<0.0001	—	95.94
B-Feed	0.0000	1	0.0000	7.29	0.0165	—	
C-Thickness of cut	0.0001	1	0.0001	41.99	<0.0001	—	1.35
A^2	0.0001	1	0.0001	40.50	<0.0001	—	1.35
Residual	0.0000	15	3.087E-06			—	—
Lack of Fit	0.0000	10	3.147E-06	1.06	0.5057	not significant	—
Pure Error	0.0000	5	2.967E-06	—	—	**R^2**	0.9937
Cor Total	0.0074	19	—	—	—	**Adj R^2**	0.9921

affected by the parameter cutting speed. However, the impact of the thickness of cut (C) and A^2 are also to a considerable extent to influence the tool wear. The observations were endorsed by the researchers B. Davoodi et al. [4].

The following mathematical model of Eq. (7) to Eq. (10) expresses the relationship between the turning parameters to the individual responses with manipulated coefficients.

Cutting tooltip temperature =

$$112.97 + 14.88A + 0.855B + \\ + 0.467C - 1.91A^2 + 1.5C^2 \quad (7)$$

Cutting force =

$$226.67 + 37.08A + 4.57B + 1.27C + \\ + 1.62AB - 31.03A^2 + 2.78B^2 \quad (8)$$

Surface roughness =

$$0.8727 + 0.1895A + 0.0284B + \\ + 0.0224C - 0.0328A^2 \quad (9)$$

Tool wear =

$$0.192 + 0.0266A + 0.0015B + \\ + 0.0036C + 0.005A^2 \quad (10)$$

Fig. 2 shows the residual plots plotted for each of the responses, most of the points were in collinear with the linear line. The alignment of the majority of points in a linear way acknowledges the fact of the adequacy of the model.

Fig. 3 displays the 3D surface graph for cutting tooltip temperature. The effects of cutting speed and feed are important to influence the cutting tooltip temperature. The graph confirms that the increment in cutting speed will greatly raise the cutting tooltip temperature, which is attributed to the fact that whenever the speed of cutting increases, the frictional force also increases between the tool and workpiece interface, thereby increasing the frictional heat. The response, cutting force was affected by the cutting speed and feed at a significant level is shown in Fig. 4. The 3D surface graph assures that the magnitude of the cutting force was increased by the higher value of cutting speed and feed. At higher cutting speed and feed, the development of built-up edge due to the severe plasticity of the chips at elevated temperature causes to increase the thrust force over the tool.

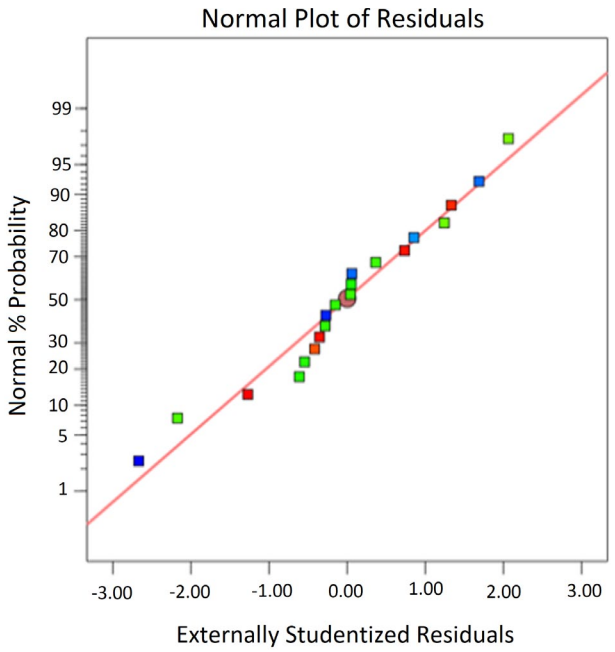

Fig. 2(a). Normal residuals plot for Cutting tooltip temperature

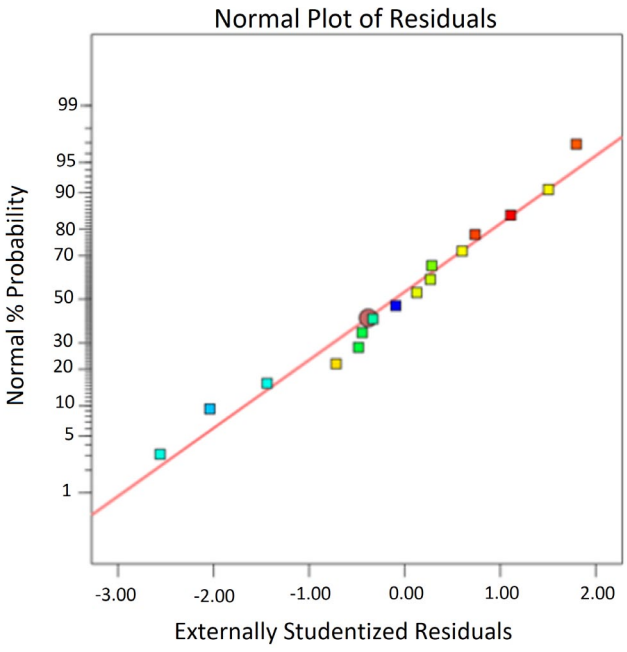

Fig. 2(b). Normal residuals plot for Surface roughness

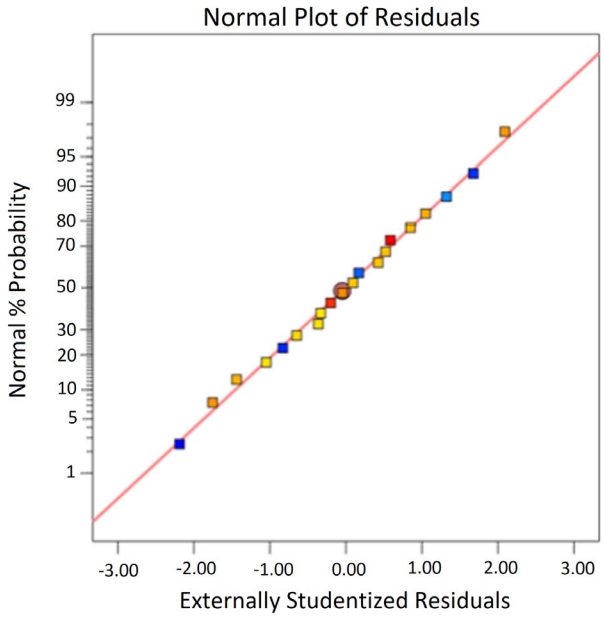

Fig. 2(c). Normal residuals plot for Cutting force

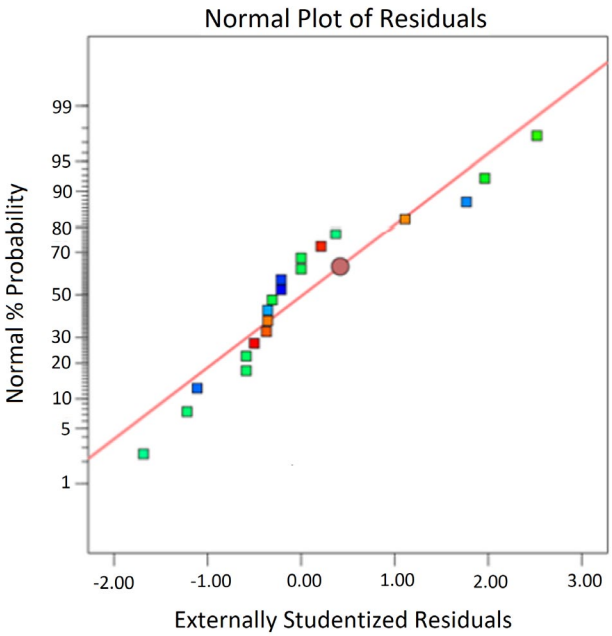

Fig. 2(d). Normal residuals plot for Tool wear

The impact of cutting speed and feed rate over the surface roughness is shown in Fig. 5 as a surface graph. At a higher level of cutting speed and feed, the development of the cutting tooltip temperature in elevated conditions is very high. The chips become more plastic and tend to weld over the workpiece material, thereby leaving the surface as more rough. The phenomenon is clearly shown in Fig. 5 by highlighting the linear relationship between cutting speed and roughness of the surface. Fig. 6 shows the surface graph for the impact of speed of cutting and thickness of cut over the tool wear. The surface seems to be curvilinear due to the quadratic model effect. It is observed that the tool wear was accelerated at a higher level of cutting speed and thickness of cut. High compressive stress and high

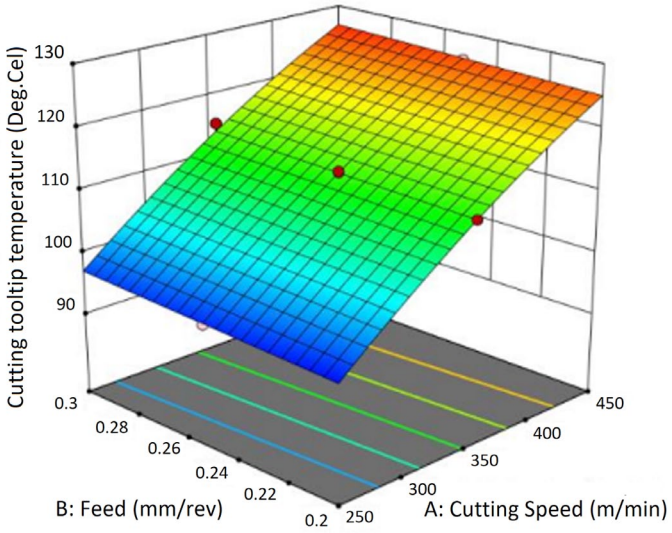

Fig. 3. Surface graph for cutting tooltip temperature

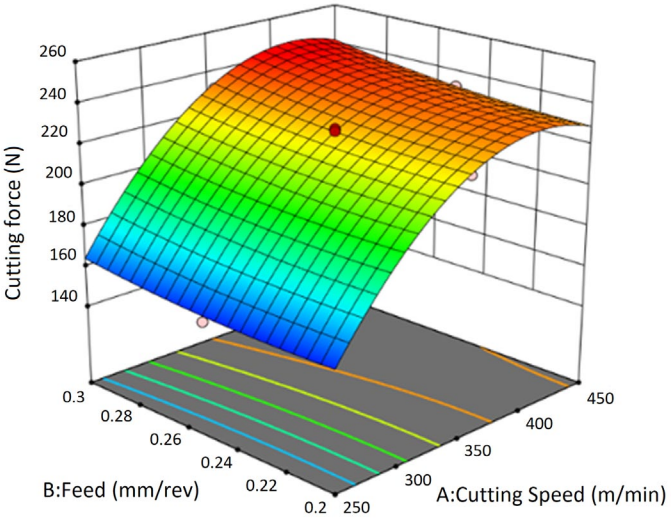

Fig. 4. Surface graph for cutting force

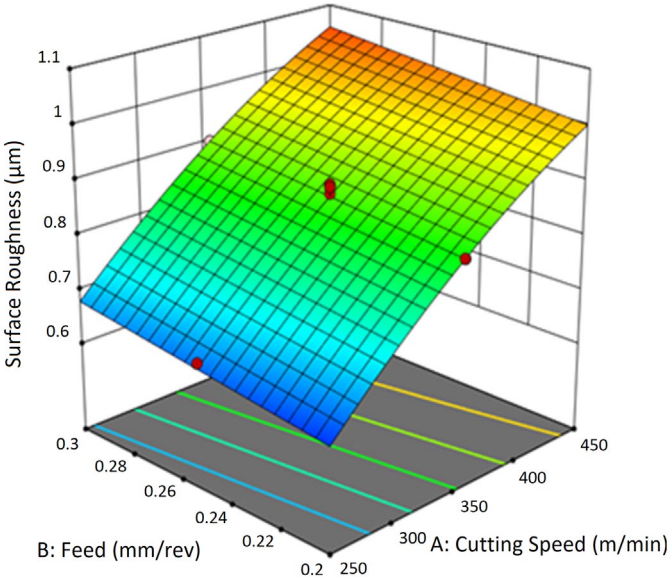

Fig. 5. Surface graph for surface roughness

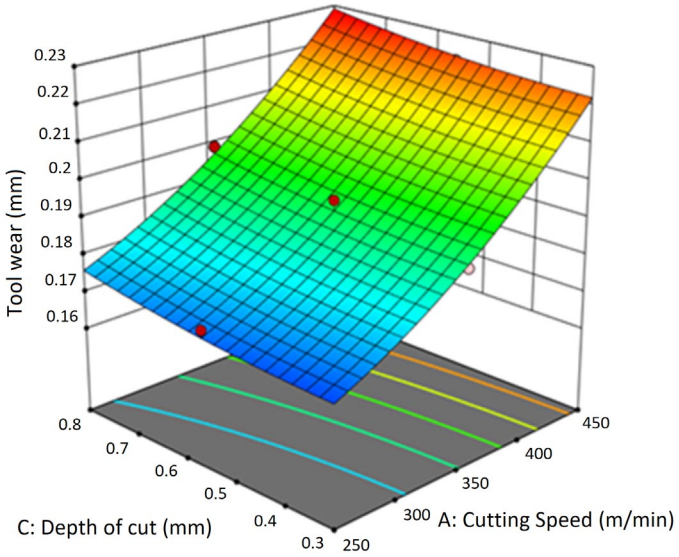

Fig. 6. Surface graph for tool wear

temperature were generated during the elevated cutting condition, which causes the tool material to thermally soften, leading to plastic deformation of the cutting edges, which accelerates the tool wear. These effects are proportionate to the increase in cutting parameters.

At a higher level of speed and thickness of cut, the rate of abrasion over the tool surface and nose portion shown in Fig. 7 was also in rapid mode, due to the excessive frictional heat. This phenomenon was linearly expressed in the surface graph.

3.2. Confirmation experiments

Another six number of experiments have been conducted to uphold the adequacy of the proposed model extensively. Out of six experiments, the first three experiments were conducted by following a design matrix, the last three experiments were conducted with the combinations which were not followed previously but within the prescribed levels.

The point prediction capability of the mathematical model was employed to predict the responses of the experiments together with 95% prediction interval. The actual and predicted mean of the four responses for the six experiments are shown in Table 7 and Table 8 respectively. The percentage of error ranges for cutting tooltip temperature, cutting force, surface roughness and tool wear are –0.42 to 1.14, –1.93 to 1.02, –2.07 to 1.64, and –0.31 to 1.54 respectively. It can be stated that the suggested model is accurate and adequate encompassing the error percentage well below 5% by maintaining the 95% prediction interval.

4. Conclusions

The innovative CNT deposited HSS tool was employed for the machining of Titanium alloy. Nearly 20 number of experiments were conducted according to RSM design matrix. Cutting force, cutting tooltip temperature, tool wear, and surface roughness were considered as the responses. The exclusively developed mathematical was used to analyze the influence of

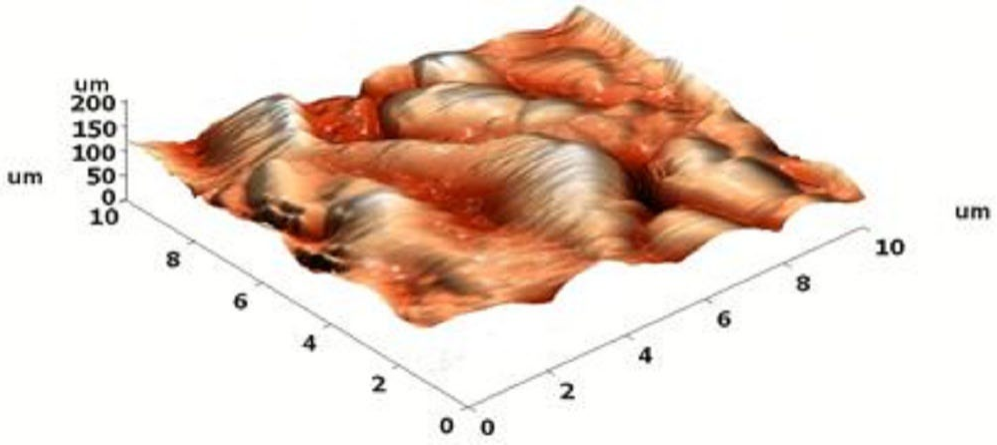

Fig. 7. AFM image of flank wear observed for CNT coated tool at level 1

TABLE 7

Confirmation experiments for cutting tooltip temperature and cutting force

S. No.	V	f	d	Cutting tooltip temperature				Cutting force			
				Actual	Predicted	Residual	% error	Actual	Predicted	Residual	% error
1	350	0.25	0.55	112.5	112.97	–0.47	–0.42	227.65	226.67	0.98	0.43
2	250	0.3	0.8	99.52	99	0.52	0.52	167.25	165.55	1.7	1.02
3	450	0.25	0.55	125.67	125.93	–0.26	–0.21	232.65	232.72	–0.07	–0.03
4	250	0.3	0.55	96	96.17	–0.17	–0.18	155.65	158.65	–3	–1.93
5	350	0.3	0.8	115.13	113.82	1.31	1.14	231.56	234.02	–2.46	–1.06
6	450	0.25	0.8	128	128.76	–0.76	–0.59	243.75	242.96	0.79	0.32

TABLE 8

Confirmation experiments for surface roughness and tool wear

S. No.	V	f	d	Surface roughness				Tool wear			
				Actual	Predicted	Residual	% error	Actual	Predicted	Residual	% error
1	350	0.25	0.55	0.878	0.8727	0.0053	0.6	0.195	0.192	0.003	1.54
2	250	0.3	0.8	0.687	0.7012	–0.0142	–2.07	0.175	0.1755	–0.0005	–0.29
3	450	0.25	0.55	1.01	1.03	–0.02	–1.98	0.223	0.2236	–0.0006	–0.27
4	250	0.3	0.55	0.661	0.6504	0.0106	1.64	0.173	0.1704	0.0026	1.5
5	350	0.3	0.8	0.901	0.9011	–0.0004	–0.04	0.193	0.1935	–0.0005	–0.26
6	450	0.25	0.8	1.09	1.08	0.01	0.92	0.228	0.2287	–0.0007	–0.31

parameters and interaction of parameters over the responses. The following important findings arrived as conclusions.

1. Adhesive strength of the deposited CNT layer was evaluated through the scratch test, and concluded that coated layer has got the sufficient adhesive strength with the substrate.
2. The proposed statistical model was validated for its adequacy through ANOVA results and normal plots.
3. The results of ANOVA and 3D surface graph revealed that the most influential parameter for the responses considered was the cutting speed. However, the impact of feed rate was at a significant level to influence the cutting force, similarly the impact of thickness of cut also at a considerable level for the tool wear.
4. The confirmation experiment results concluded that the model has experienced a percentage of error calculated between predicted and actual mean, well below the allowable limit of 5% subject to the 95% confidence interval level.
5. The proposed model can be helpful to propose the optimized parameter level to achieve the required customized response value.

REFERENCES

[1] C. Machai, D. Biermann, J. Mater. Process. Technol. **211** (6), 1175-1183 (2011), doi:10.1016/j.jmatprotec.2011.01.022

[2] H. Bensouilah, H. Aouici, I. Meddour, M.A. Yallese, T. Mabrouki, F. Girardin, Measurement **82**, 1-18 (2016), doi:10.1016/j.measurement.2015.11.042

[3] K. Bouacha, M.A. Yallese, T. Mabrouki, J.F. Rigal, Int. J. Refract. Met. Hard Mater. **28** (3), 349-361 (2010), doi:10.1016/j.ijrmhm.2009.11.011

[4] B. Davoodi, B. Eskandari, Measurement **68**, 286-294 (2015), doi:10.1016/j.measurement.2015.03.006

[5] J.S. Dureja, R. Singh, M.S. Bhatti, Prod. Manuf. Res. **2** (1), 767-783 (2014), doi:10.1080/21693277.2014.955216

[6] A.J. Makadia, J.I. Nanavati, Measurement **46** (4), 1521-1529 (2013), doi:10.1016/j.measurement.2012.11.026

[7] M. Nalbant, H. Gökkaya, G. Sur, Mater. Des. **28** (4), 1379-1385 (2007), doi:10.1016/j.matdes.2006.01.008

[8] M.Y. Noordin, V.C. Venkatesh, S. Sharif, S. Elting, A. Abdullah, J. Mater. Process. Technol. **145** (1), 46-58 (2004), doi:10.1016/s0924-0136(03)00861-6

[9] A.P. Paiva, J.R. Ferreira, P.P. Balestrassi, J. Mater. Process. Technol. **189** (1-3), 26-35 (2007), doi:10.1016/j.jmatprotec.2006.12.047

[10] A.K. Sahoo, B. Sahoo, Measurement **45** (8), 2153-2165 (2012), doi:10.1016/j.measurement.2012.05.015

[11] B. Pazhanivel, T.P. Kumar, G. Sozhan, Mater. Sci. Eng. B **193**, 146-152 (2015), doi:10.1016/j.mseb.2014.12.006

[12] A. Hirata, N. Yoshioka, Tribol. Int. **37** (11-12), 893-898 (2004), doi:10.1016/j.triboint.2004.07.005

[13] T. Borkar, S. Harimkar, Surf. Eng. **27** (7), 524-530 (2011), doi:10.1179/1743294410y.0000000001

[14] J.P. Salvetat, J.M. Bonard, N.H. Thomson, A.J. Kulik, L. Forro, W. Benoit, L. Zuppiroli, Appl. Phys. A **69** (3), 255-260 (1999), doi:10.1007/s003399900114